

Experimental and computational analysis of springback in dual phase steels

Análisis experimental y computacional de la recuperación elástica en aceros bifásicos

Y. Parra-Rodríguez ; J. M. Arroyo-Osorio ; R. Rodríguez-Baracaldo 

DOI: <https://doi.org/10.22517/23447214.24513>

Artículo de investigación científica y tecnológica

Abstract— In this work the comfortability of dual-phase automotive steel DP600 is studied through uniaxial tensile tests and V-die bending tests in different directions relative to the rolling direction. A microstructural analysis was also carried out in each characteristic region of the deformation zone, evidencing the changes in the morphology of the microstructure grains. Additionally, the plastic anisotropy of the material was studied by implementing the constitutive anisotropy models known as Hill-48 and Barlat-89. The results showed an increase in elastic recovery at 45 ° and 90 ° from the rolling direction. This variation can be attributed to the morphology of the martensite that created preferential location zones within the material during the rolling process. The two models Hill-48 and Barlat-89 correctly describe the yield surface and the plastic anisotropy obtained in the experimental tests carried out. The simulation using the finite element method and the Hill-48 model gave satisfactory results in the prediction of the elastic recovery as compared to the experimental results obtained with the V-die bending test.

Index Terms— Anisotropy, Dual phase steels, Springback, Yield criterion

Resumen—En este trabajo se estudia la confortabilidad del acero automotriz de fase dual DP600 mediante ensayos de tracción uniaxial y ensayos de doblado en V en diferentes direcciones relativas a la dirección de laminación. También se realizó un análisis microestructural en cada región característica de la zona de deformación, evidenciando los cambios en la morfología de los granos de la microestructura. Adicionalmente, se estudió la anisotropía plástica del material implementando los modelos constitutivos de anisotropía conocidos como Hill-48 y Barlat-89. Los resultados mostraron un aumento de la recuperación elástica a 45 ° y 90 ° de la dirección de laminado. Esta variación se puede atribuir a la morfología de la martensita que creó zonas preferenciales de ubicación dentro del material durante el proceso de la laminación. Los dos modelos Hill-48 y Barlat-89 describen de manera correcta la superficie de fluencia y la anisotropía plástica obtenida en los ensayos experimentales realizados. La simulación mediante el método de elementos finitos y el modelo Hill-48 arroja resultados satisfactorios en la predicción de la recuperación elástica ajustándose a los resultados experimentales obtenidos con la prueba de doblado en V.

Palabras claves— Anisotropía, Aceros bifásicos, Recuperación elástica, Criterio de fluencia.

I. INTRODUCTION

GIVEN their high strength and low comparative weight, so-called advanced high-strength steels (AHSS) and ultra-high-strength steels (UHSS) are frequently used in the automotive industry as a material for various vehicle components. Specifically, in the AHSS category, dual-phase steels (DP) have been used as material for structural parts of vehicles, with the objectives of improving safety in collisions and reducing weight, with the consequent reduction in fuel consumption and therefore in polluting emissions. The manufacture of components with DP steels is generally carried out by forming steel sheets. Being then the conformability one of its most relevant characteristics.

The microstructure of DP steels is generally characterized by having a ferrite matrix with homogeneously distributed martensite islands [1]-[3]. The combination of the ductile and soft phase of ferrite with the brittle and hard phase of martensite, produces an acceptable formability. However, one of the main difficulties in forming DP steel sheets is the springback or elastic recovery phenomenon. The springback effect is the elastic change that occurs in the geometry of the component when the respective forming tooling is removed. This effect has been explained mainly by the state of stresses resulting at the end of the deformation process. Although it is possible to try to consider the effect of springback in the design phase of the forming process, this effect generally originates additional process operations, with associated cost overruns [4].

Bending is a manufacturing process in which a sheet, generally made of metal alloy, is transformed from a flat geometry into a geometry with a preset profile. In this process, the sheet is bent sequentially, thanks to the force and movement applied by brake tooling. The springback or elastic recovery effect is quantified as the relationship between the preset angle in the design, and the angle obtained in the bent sheet after removing

This manuscript was sent on October 05, 2020 and accepted on June 02, 2021. This work was supported by Universidad Nacional de Colombia.

Y. Parra-Rodríguez is with Universidad Nacional de Colombia, Car 30 No 45-03, Bogotá D.C, Colombia (e-mail: yeparraro@unal.edu.co).

J. M. Arroyo-Osorio is with Universidad Nacional de Colombia, Car 30 No 45-03, Bogotá D.C, Colombia (e-mail: jmarroyoo@unal.edu.co)

R. Rodríguez-Baracaldo is with Universidad Nacional de Colombia, Car 30 No 45-03, Bogotá D.C, Colombia (e-mail: rodriguezba@unal.edu.co)



the brake tooling. Several researchers have worked on the springback effect and as a result, they have proposed different analytical models, or performed systematic experiments, or developed models using computational mechanics. The variables considered have generally been the final geometry, the properties of the material and the parameters of the forming process [4].

To study and experimentally characterize springback in sheet metal forming, the most used techniques include U-die bending, V-die bending, and cylindrical bending. The main advantage of these three methods is that the elastic recovery levels obtained can be easily measured. The sensitivity to elastic recovery is defined based on the input parameters of relation between the tool radius and sheet material thickness (R/t), the mechanical properties of the material and the contact parameters. The major disadvantage of those experiments is that several of the actual conditions of the sheet metal forming process are not reproduced [5]-[10].

The first elastic recovery models were made using the classical analytical methods of materials mechanics. The analytical solution for a pure bending test, for a perfect elastic-plastic material, with a known R/t ratio (radius of curvature / thickness), was established by several authors [11][12]. Other developments include analysis of bending combined with traction, introducing the effects of elastic coefficient, thickness, strain hardening, yield limit and Young's modulus [13][14].

Other authors have used the finite element method (FEM) to model the springback, with the intention of determining the necessary changes in the geometry of the brake tools, in such a way that the piece obtained has the required geometry, after completing its elastic recovery. It should be noted that the initial results were not very accurate. Precise estimation of springback using FEM essentially depends on applying a correct model of the material [15]. This need led to new developments, for example, the use of the Bauschinger effect and other more complex models [16][17]. It should be noted that the more precise the FEM models are, the more input parameters are needed, so that they can adequately describe the stress state, and for this, more complex experimental tests are needed [18]-[25].

With the aim of contributing to the understanding of springback in dual-phase AHSS, in this work a simplified mechanical characterization has been carried out, and its conformability has been studied. For this, experimental V-die bending tests were carried out, and a numerical model was tested, based on the Hill-48 and Barlat-89 plasticity models.

II. EXPERIMENTAL PROCEDURE

A DP600 dual phase steel with 3.5 mm thickness was selected for this research. Its chemical composition has determined by optical emission spectroscopy is shown in Table I.

TABLE I.
CHEMICAL COMPOSITION OF DP STEEL.

Element	C	Si	Mn	S	Fe
Mass %	0.069	0.688	1.216	0.007%	Balance

Tensile strength tests were used to characterize the mechanical properties, according to the ASTM E-8 standard test [26]. The specimens were cut using a water jet process, with orientations of 0, 45 and 90 degrees with respect to the rolling direction, see Fig. 1. The dimensions and photographs of the specimens are shown in Fig. 2.

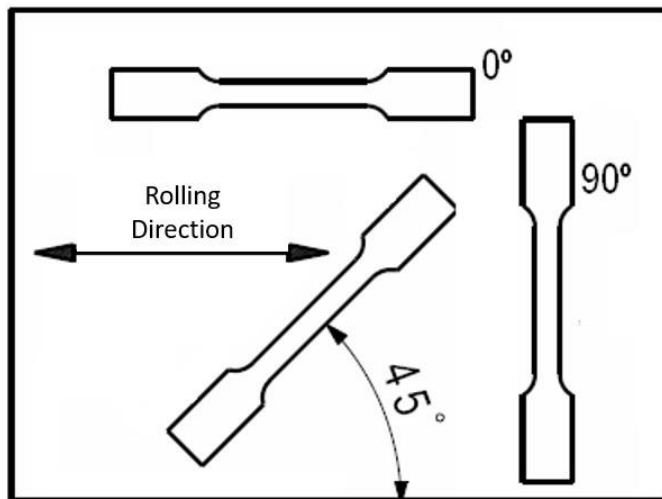


Fig. 1. Orientation for specimens cutting.

Quasi-static tensile tests were performed in a universal test machine, Shimadzu UH-X of 50 tons using a head speed of 0,01 mm/s. To determine the plastic anisotropy r , it was used the standard test ASTM E-517 [27]. Once cut the specimens, different measurements of width and thickness were taken, with a digital micrometer, to have adequate accuracy in the obtention of the plastic anisotropy coefficient. The plastic anisotropy coefficient r was determined as the ratio between the width strain and the strain in the longitude after the material has been deformed, as shown in (1). During the deformation, it is assumed that the volume of the specimen remains constant and for this reason, the change in thickness can be calculated from the change in longitude and width.

$$r = \frac{\ln(w_o/w_f)}{\ln(l_f w_f / l_o w_o)} \quad (1)$$

Where l_o is the original longitude, l_f the final longitude, w_o original width and w_f the final width. The test was performed with a head speed of 0,001 mm/s, taking pre-deformed specimens of 8% following the recommendation by Chongthairungruang et al. [7] in the determination of r value in low carbon steels.

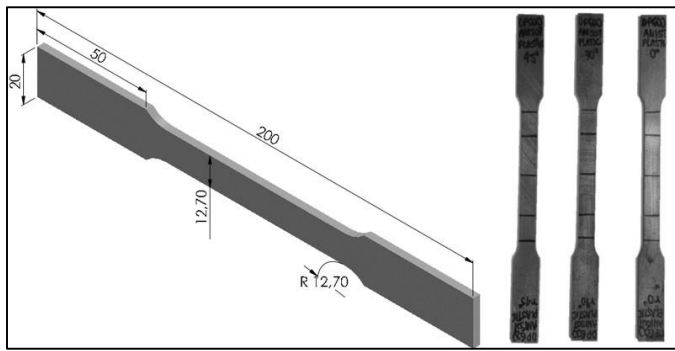


Fig. 2. Dimensions and photographs of DP steel specimens.

To study the springback, V-die bending tests were performed in a bending machine Ermak HAP 2680. The specimens for this test were cut in the three directions mentioned above. These specimens have a rectangular shape of 100 mm x 20 mm and the geometry in the matrix has a bending angle of 85 degrees and a radius of curvature of 2.5 mm, see Fig. 3. The springback angle (θ) of the specimens was measured on photographs taken after the load by using a graphic editor, and verified with a protractor Mitutoyo S-187, which has an accuracy of ± 5 min.

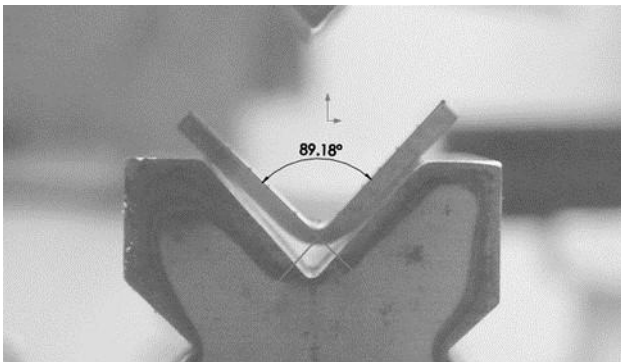


Fig. 3. Photography of V-die bending test.

The springback K in (2) was calculated as the ratio between the initial angle ($\theta_{initial}$), and the final angle (θ_{final}) in that way the conformability of the material can be evaluated.

$$K = \frac{\theta_{inicial}}{\theta_{final}} \quad (2)$$

In order to evaluate the microstructure of the material, metallography specimens were taken both before and after the bending process, near the curvature region in different directions. The metallographic polish was made with alumina following an etching step with Nital 2% for 5 seconds. The metallography specimens were observed with a scanning electron microscope FEI-Quanta 200 and with an optical microscope LECO AI32.

The volumetric fraction of both ferritic and martensitic phases was determined according to the standard ASTM E1245 [28]. The method applied use photomicrography taken with the optic microscope. To determine the percent by volume of the martensitic phase, it was used the Image-J software.

The numeric model of the experiment was developed in the ANSYS V19 ACADEMIC software [29]. Specifically, the APDL mechanic module was used to calculate the springback using the angles in the die and in the deformed sheet. Hill-48 model was used to predict the springback.

III. YIELD MODELS AND CRITERIONS

In pursuance of the analysis of the material, were considered both the Hill yield criterion and the Barlat-89 yield criterion.

A. Hill yield criterion

The Hill yield criterion, also named as Hill-48, is one of the most common yield criteria [18]. This criterion (3) is frequently used in the modeling of forming processes, and it do not consider the material microstructure. Furthermore it is a quadratic function where F, G, H, L, M and N are constants that describe the anisotropy of the material, x, y, z are the orthogonal axis of anisotropy in which the properties have double symmetry and thus the xy, zx and yz are the symmetry planes. Under plane stress state, the yield quadratic function of Hill-48 can be written as in (3).

$$2f(\sigma_{ij}) = F(\sigma_y - \sigma_z)^2 + G(\sigma_z - \sigma_x)^2 + H(\sigma_x - \sigma_y)^2 + 2L\tau_{yz}^2 + 2M\tau_{zx}^2 + 2N\tau_{xy}^2 = 1 \quad (3)$$

The relation between the anisotropy coefficients ($r_0, r_{45}, y r_{90}$) and the coefficients $F, G, H,$ and N are showed in (4) to (7).

$$F = \frac{r_0}{(1 + r_0)r_{90}} \quad (4)$$

$$G = \frac{1}{(1 + r_0)} \quad (5)$$

$$H = \frac{r_0}{(1 + r_0)} \quad (6)$$

$$N = \frac{(1 + 2r_{45})(r_0 + r_{90})}{2(1 + r_0)r_{90}} \quad (7)$$

B. Barlat-89 yield criterion

Barlat-89 yield criterion model is a generalization of the Hosford yield criterion [19] by extending it in an x, y, z coordinate system and represents the state of plane stress for yield surface with (8).

$$f = a|K_1 + K_2|^M + a|K_1 - K_2|^M + c|2K_2|^M = 2\sigma_e^M \quad (8)$$

In (8), σ_e is the yield strength in a uniaxial tension state. K_1 and K_2 are invariants of the stress tensor while M is an integer exponent having the same significance as the exponent a used by Hosford, see (9) to (12).

$$K_1 = \frac{\sigma_{11} + h\sigma_{22}}{2}, K_2 = \sqrt{\left(\frac{\sigma_{11} + h\sigma_{22}}{2}\right)^2 + p^2\sigma_{12}^2} \quad (9)$$

$$a = 2 - c = 2 - 2 \sqrt{\frac{r_0}{1+r_0} \frac{r_{90}}{1+r_{90}}} ; \quad (10)$$

$$h = \sqrt{\frac{r_0}{1+r_0} \frac{1+r_{90}}{1+r_0}} ; \quad (11)$$

$$p = \frac{\sigma_e}{\tau_{s1}} \left(\frac{2}{2a + 2^M c} \right)^{\frac{1}{M}} \quad (12)$$

The parameters a and c in (8) and h in (9) are material constants that can be determined from uniaxial tensile tests in the 0° , 45° and 90° directions. The exponent M is related to the crystallographic structure, in this case the value is 6 according to several works [20]-[22][25], because the dual phase steels have a BBC structure. And the coefficient p must be calculated by a numerical procedure or by using (10) to (12). For $\sigma_{12}=0$, (8) and (9) are practically reduced to the Hosford yield criterion in principal stresses.

IV. RESULTS AND DISCUSSION

Fig. 4 shows the stress-strain curves obtained from the uniaxial tensile test, considering the direction respecting the rolling direction 0, 45 and 90 degrees. Table 2 shows the variations of the yield strength 0.2% in the different directions mentioned above. The increase in the yield strength at 45° compared to the 0° direction agrees to the one reported by Ozturk et al. [20] y Sarraf & Green [16] where DP600 steels are studied. Table II also shows the plastic anisotropy coefficients R-Values, calculated to a deformation of 8%, within the limit range between yield and ultimate strength.

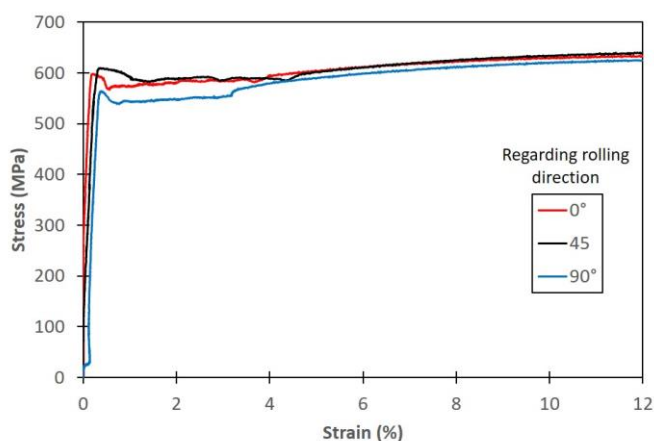


Fig. 4. Experimental strain-stress curve of DP steel.

TABLE II
EXPERIMENTAL YIELD STRENGTH AND R-VALUE OF DP STEEL.

Direction	Yield Strength (MPa)	R-value
Rolling direction (0°)	597,67	0,855
Diagonal direction (45°)	610,28	0,864
Transversal direction (90°)	593,44	0,933

Table III shows the measured values of the final angle after the bending and the calculated values of the springback. It can be observed that the final forming angle is greater at 45° and 90° degrees. According to (2), the values of springback must be less for 45° and 90° samples at. Haus [21] and Dos Santos [30], using the V-die bending test with DP800, TRIP800 and HSLA450, also reported lower values of the springback angle in the 45° and 90° directions.

TABLE III
SPRINGBACK IN EACH DIRECTION FOR DP STEEL.

Direction	Average final angle ($^\circ$)	Springback
Rolling direction (0°)	89.20	0.953
Diagonal direction (45°)	90.23	0.942
Transversal direction (90°)	90.19	0.942

Fig. 5 shows the SEM image of the microstructure of DP steel without deformation. The grey dark area corresponds to the ferritic phase and the lighter regions are martensitic phase, which have a uniform appearance with a low percentage of volumetric fraction; besides martensitic phase can be seen as a net surrounding the ferritic phase.

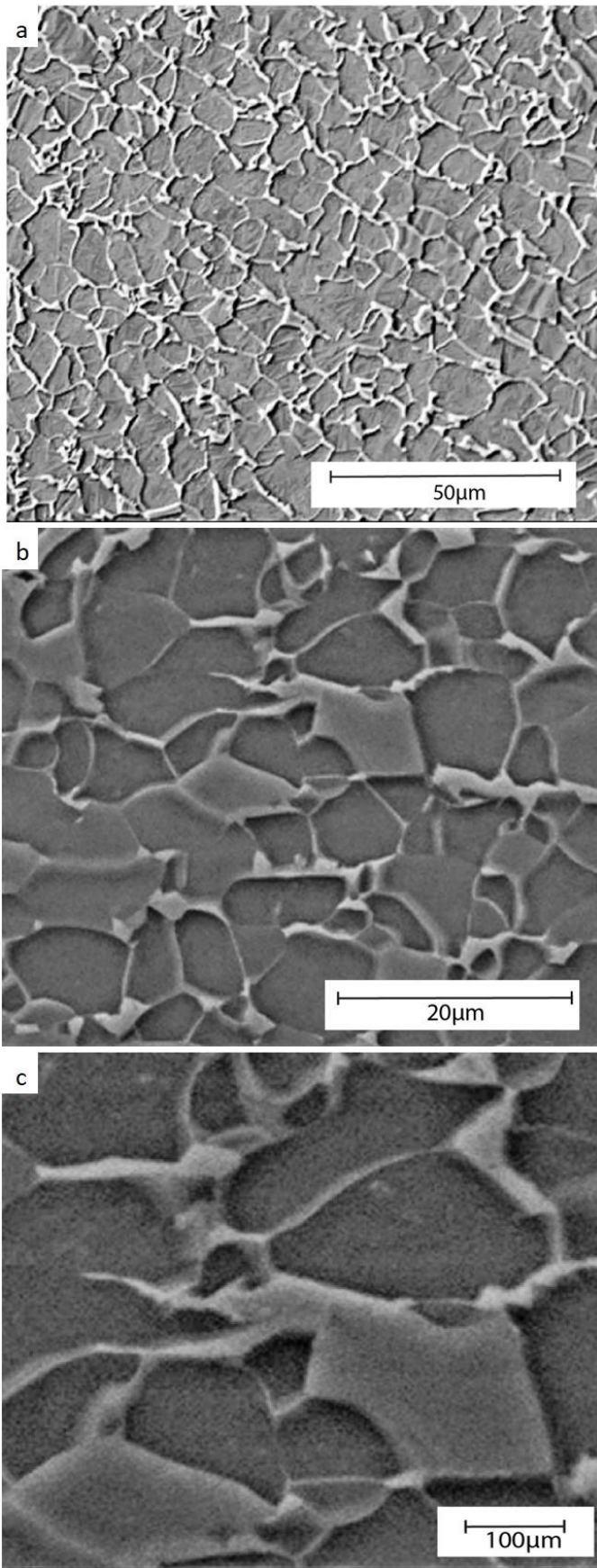


Fig. 5. SEM images of the DP600 Steel microstructure, (a) 2000X, (b)5000X, (c) 10.000X.

Fig. 6 shows a representative example of the work carried out with the image software to determine the volumetric fraction of both phases, obtaining 20% of martensite.

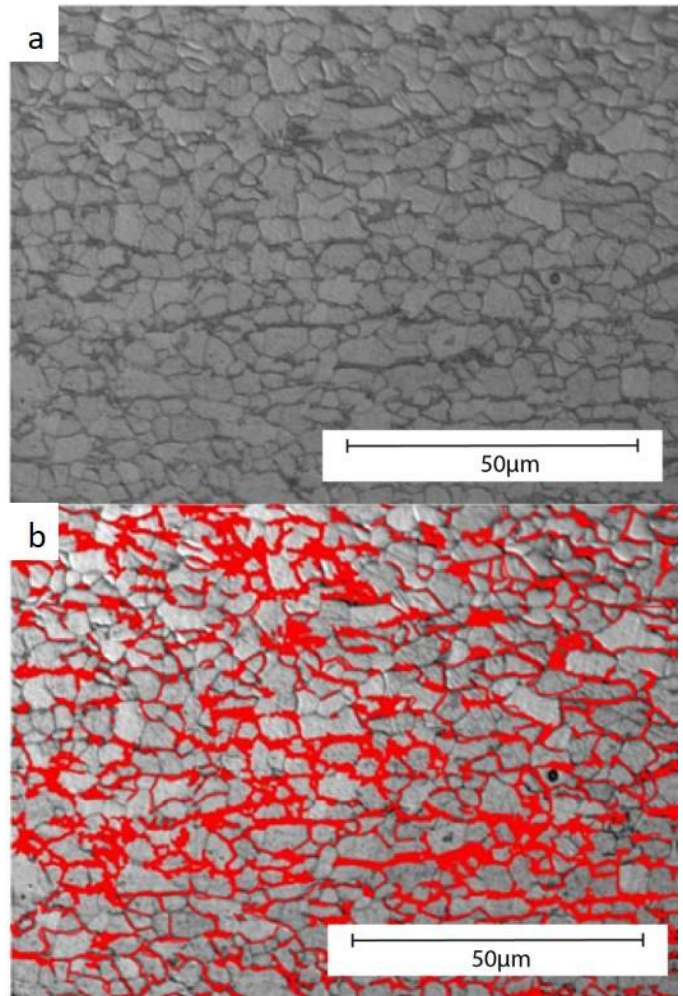


Fig. 6. Example of measurement of volumetric fraction of martensite in DP600 Steel, (a) optical micrography, (b) optical micrography plus image software analysis.

The images taken with the optical microscope in the deformed region (curved zone) in the 0°, 45° and 90° specimens, were analyzed after the V-die bending. Fig. 7 indicates the zone under compression stress, the zone under tensile stress, the neutral axis and the points where the metallography was taken.

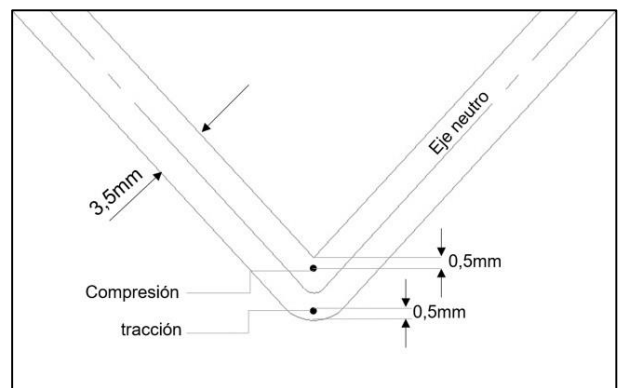


Fig. 7. Points where the metallography was taken.

Fig. 8 shows the metallographies of the 0°, 45° and 90° specimens. In all cases, it can be seen that the two phases have been plastically deformed, furthermore in the compressive zones, the ferritic grains took symmetric shape, and the martensitic phase also was deformed to border the ferritic. On the other hand, in the tensile zones, the martensitic and the ferritic phases were elongated in the direction of the load. In Haus [21] and Dos Santos [30], a similar deformation was reported for dual phase steels and transformation induced plasticity steels TRIP. In the other hand, there were no evidence of micro-cracks due to the tensile load. The ductility of the steel evidenced in the stress-strain curve (Fig. 4), may explain the absence of micro-cracks.

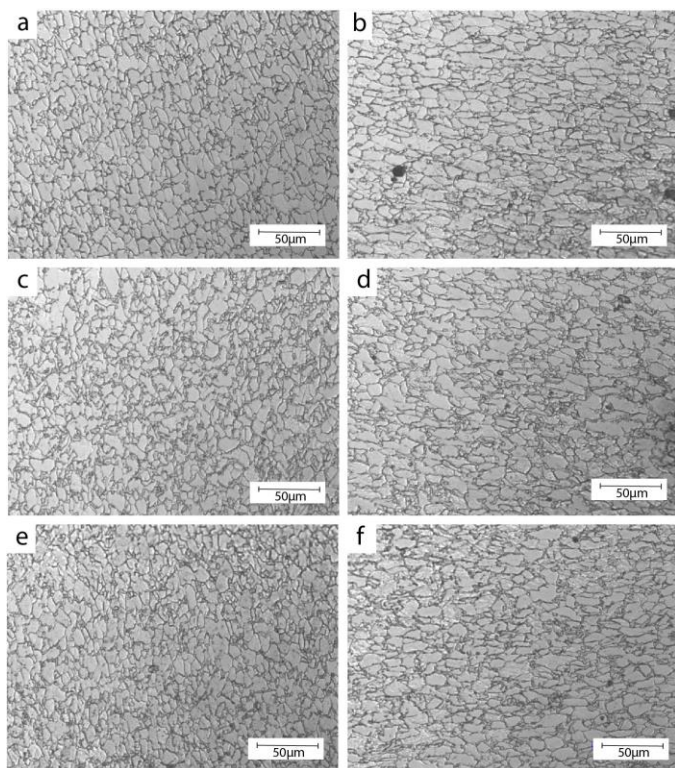


Fig. 8. Optical micrographies of DP steels with a V-die bending, (a) compression zone 0°, (b) tensile zone 0°, (c) compression zone 45°, (d) tensile zone 45°, (e) compression zone 90°, (f) Tensile zone 90°.

V. PREDICTION OF YIELD STRENGTH, ANISOTROPY COEFFICIENTS AND YIELD SURFACE.

The estimations of the yield strength (σ_y) under the models of Hill-48 and Barlat-89 are shown in the Fig. 9, and they are compared with the experimental results of the uniaxial tensile tests at 0°, 45° and 90°. The yield functions were calculated using (3) and (8), with the anisotropy coefficients obtained by the experimental test. The results show that the Hill-48 criterion and Barlat-89 criterion are very accurate in the 0° direction, giving a relative error of 0,1% in both cases. On the contrary, the criterions in the 45° and 90° directions, are less exact, giving a relative error of 5,4% for the perpendicular case, and 1,43% for the diagonal direction.

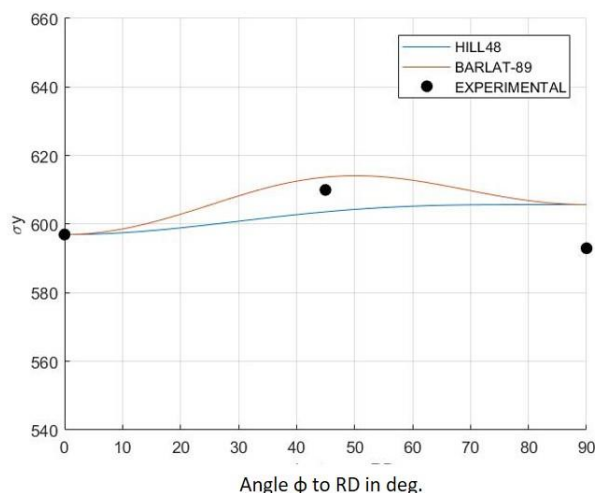


Fig. 9. Experimental and estimated yield strength considering the rolling direction RD.

The estimation of the anisotropy values (r_ϕ) was made with Barlat-89 and Hill-48 criterions. Fig. 10 shows a comparison with the experimental results. The Hill-48 model has a relative error of 0,1% in (r_ϕ) in comparison with the 20% relative error obtained with the Barlat-89 model. This can be explained by the fact that the Barlat-89 model requires only two parameters of plastic anisotropy (r_0 and r_{90}) while Hill-48 yield criterion needs three parameters in its quadratic equation (r_0 , r_{45} and r_{90}). Similar results were obtained by Hou et al. [8] and Ozturk et al. [20]. It must be mentioned that in these studies are reported many results that allow the models to be better adjusted.

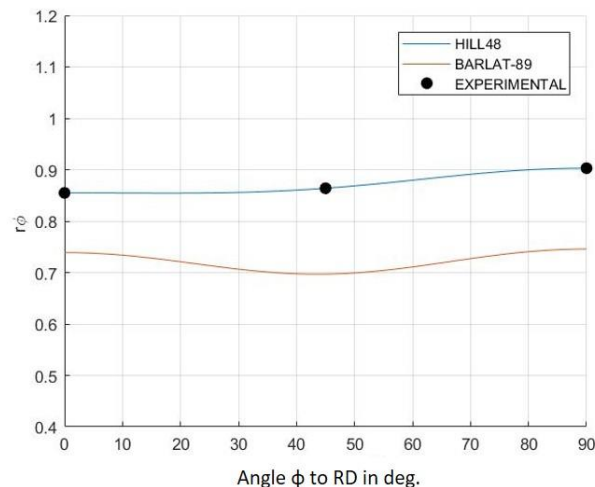


Fig. 10. Experimental and estimated anisotropy coefficient considering the rolling direction RD.

Table 4 shows the calculated anisotropic constants F , G , H , and N of Hill-48 yield criterion. Table 4 also shows the calculations of the constants a , c , h and p in the case of Barlat-89 non-quadratic function, taking the shear stress as a constant, namely $\sigma_{12} = 0$ in a normalized form.

TABLE IV
CALCULATED ANISOTROPY CONSTANTS FOR HILL-48 AND BARLAT-89 CRITERIONS.

Hill-48				
Material	<i>F</i>	<i>G</i>	<i>H</i>	<i>N</i>
DP600	0,494	0,539	0,461	1,409
Barlat-89				
Material	<i>a</i>	<i>c</i>	<i>h</i>	<i>p</i>
DP600	1,706	0,935	0,986	0,950

Fig. 11 shows the yield surfaces calculated with Hill-48 and Barlat-89 quadratic models, evidencing some differences in the behavior for the analyzed DP material. Hill-48 yield function occupies a slightly narrower area than Barlat-89 yield function. Also, the Barlat-89 model offers a closer estimation of the yield strength as compared with the Hill-48 model. Eggertsen and Mattiasson [23] also reported the advantage of Hill-48 in front of BBC-2000 and Barlat-89 models.

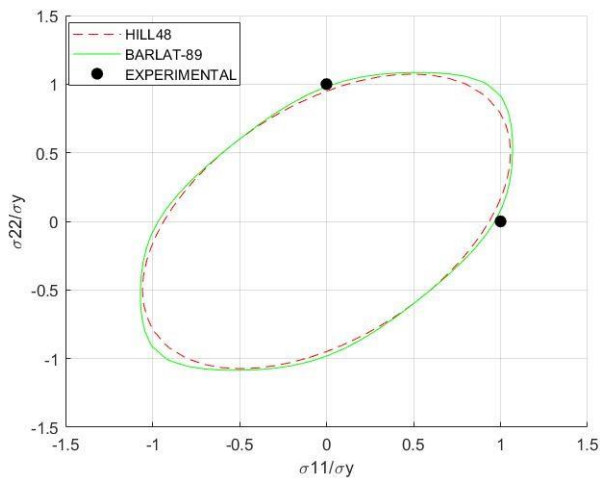


Fig. 11. Estimation of the yield surfaces using Hill-48 and Barlat-89 criterions.

VI. SIMULATION OF SPRINGBACK IN DP STEEL

In sheet metal working is necessary to plastically deform the raw material, for this reason the material properties, especially the stress-strain relationship, must be characterized with accuracy so it can be used in numerical analysis of the stamping process. This relationship was born out of the necessity to describe with constitutive models for anisotropic materials, the yield surface as a primordial and necessary element in the study of a metal sheet. To modeling the sheet working in the DP600 steel, it was used ANSYS V19 ACADEMIC software [29]. Specifically using the modulus mechanical APDL to estimate the final shape of the samples after the tool away. Plane 182 element (4 nodes) was used employing displacements in the UX and UY directions. The mesh convergency analysis was carried out with an error less than 1% and 1150 nodes.

The model, the boundary conditions and the restrictions for the FEM simulation were generated according to the experimental

setup in the V-die bending process. The input data for the simulation were geometric conditions, mechanical properties of the DP steel, tools displacements and contacts. Additionally, the tool was treated as a rigid body, while the sheet and the matrix were treated as a deformable body. The tool moves applying the load and then returns to its original position.

Fig. 12 shows the simulation results. Von Mises equivalent stress and strain were obtained for the DP steel from initial state until tool displacement of 17.4 mm. As expected, the region around the radius of the matrix or sheet curvature shown greater stress, a critic phenomenon for the springback effect.

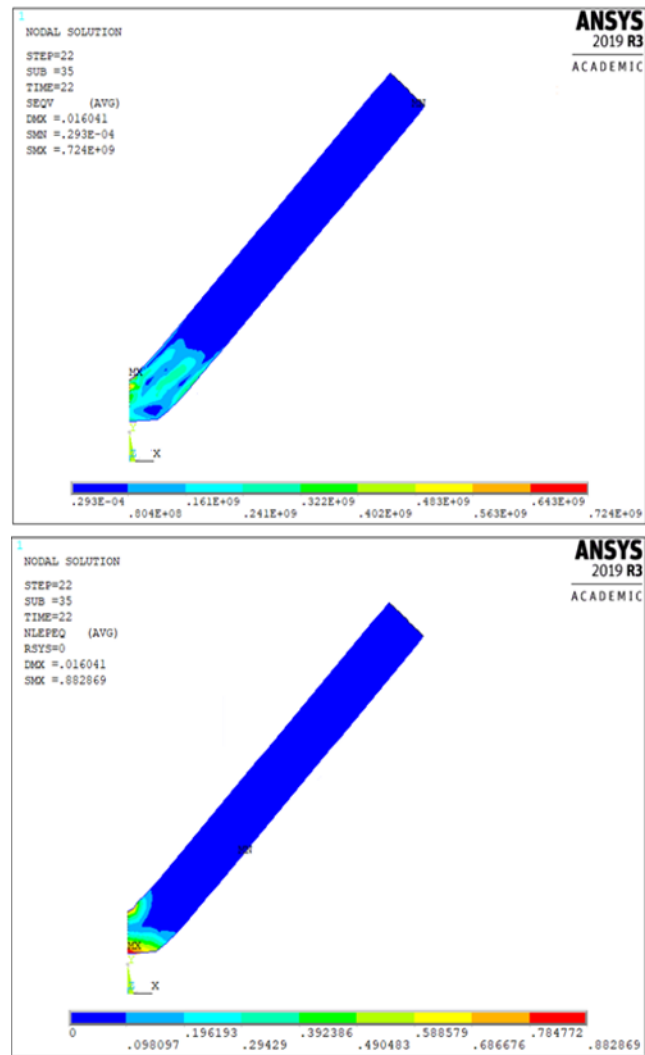


Fig. 12. FEM analysis of the springback, (a) Von Mises equivalent stress, (b) Von Mises equivalent strain.

In order to compare the numerical and experimental results appropriately, the final geometry after V-die bending process and springback was exported and the final angle was measured with an image analyzer software, see results in Fig. 13.

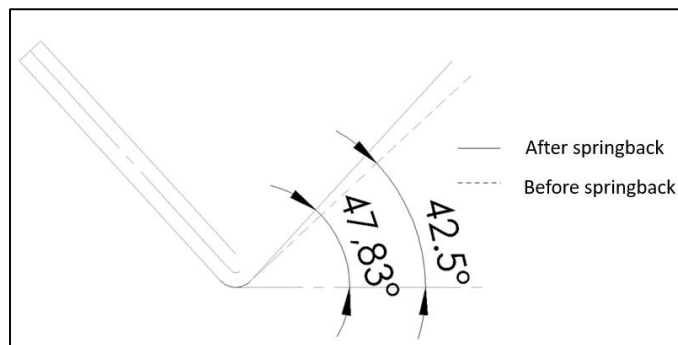


Fig. 13. Measured springback angles in the FEM model.

The simulation results of springback angle were also determined with the Hill-48 yield criterion at the rolling direction. This angle value presented a relative error of 5,4% compared with the experimental result. This level of error is acceptable but higher than other reports. Konzack et al. [24] reported that the geometrical parameters influence the springback and demonstrated that the Hill-48 model has a satisfactory estimation of verticality of walls in a rail bending test for DP and TRIP steels.

In future work it is going to be included the cinematic hardening as well as plastic and elastic properties when the material is loaded-unloaded (Bauschinger effect). These new considerations will presumably allow obtaining results closer to the real behavior of the material.

VII. CONCLUSIONS

A methodology was implemented to evaluate and estimate springback in DP600 dual phase steels supported by conventional experimental methods and finite element method modeling. In light of the results obtained, it can be affirmed that the studied steel presented higher springback at 45° and a at 90° than at 0° in relation with the rolling direction. This variation can be attributed to the morphology of the martensite that created preferential location zones within the material during the rolling process.

The implemented constitutive models of anisotropy (Hill-48 and Barlat-89 yield criterions) described in a correct way the yield surface and the plastic anisotropy obtained in the performed experimental tests. Hill-48 better estimated the anisotropy coefficient, while Barlat-89 described more accurately the yield surface.

FEM modeling and the Hill-48 model gave correct results in the springback prediction as compared with the experimental results obtained with the V-die bending test.

ACKNOWLEDGMENTS

The authors thank the financial support provided by Universidad Nacional de Colombia, as well as the support of laboratories from the Mechanical and Mechatronics Engineering Department on the development of this work.

REFERENCES

- [1] R. W. Logan, y W. F. Hosford, "Upper-bound anisotropic yield locus calculations assuming $\langle 111 \rangle$ -pencil glide." *International Journal of Mechanical Sciences*, vol. 22, no. 7, pp. 419-430, 1980 DOI: 10.1016/0020-7403(80)90011-9
- [2] M. Kleiner, M. Geiger, y A. Klaus, "Manufacturing of Lightweight Components by Metal Forming." *CIRP Annals*, vol. 52, no. 2, pp. 521-542, 2003. DOI: 10.1016/S0007-8506(07)60202-9
- [3] H. Hayashi, y T. Nakagawa, "Recent trends in sheet metals and their formability in manufacturing automotive panels," *Journal of Materials Processing Technology*, vol. 46, no. 3, pp.455-487, 1994. DOI: 10.1016/0924-0136(94)90128-7
- [4] R. H. Wagoner, H. Lim, y M. G. Lee, "Advanced Issues in springback," *International Journal of Plasticity*, vol. 45, pp. 3-20, 2013. DOI: 10.1016/j.ijplas.2012.08.006
- [5] D. Banabic, "Plastic Behaviour of Sheet Metal," *En D. Banabic* (Ed.), *Sheet Metal Forming Processes: Constitutive Modelling and Numerical Simulation* (pp. 27-140). Springer. 2010. DOI: /10.1007/978-3-540-88113-1_2
- [6] I. Burchitz. "Springback, improvement of its predictability: Literature study report Netherlands Institute for Metals Research," 2005
- [7] B. Chongthairungruang, V. Uthaisangsk, S. Suranuntchai, y S. Jiratharanat, "Experimental and numerical investigation of springback effect for advanced high strength dual phase steel," *Materials & Design*, vol. 39, pp. 318-328, 2012. DOI: 10.1016/j.matdes.2012.02.055
- [8] Y. Hou, J. Min, J. Lin, Z. Liu, J. E. Carsley, & T. B. Stoughton, "Springback prediction of sheet metals using improved material models," *Procedia Engineering*, vol. 207, pp. 173-178. 2017. DOI: 10.1016/j.proeng.2017.10.757
- [9] S. Toros, A. Polat, y F. "Ozturk, Formability and springback characterization of TRIP800 advanced high strength steel," *Materials & Design*, vol. 41, pp. 298-305, 2012. DOI: 10.1016/j.matdes.2012.05.006
- [10] F Gardiner. "The Springback of Metals," *Asme*, vol. 79, no. 1, pp. 1-9. 1957.
- [11] R. Queener. "Elastic springback and residual stresses in sheet metal formed by bending," *Asme*, vol. 61, no. 1, pp. 757-768. 1968.
- [12] K. C. Chan, y S. H. Wang, "Theoretical analysis of springback in bending of integrated circuit leadframes," *Journal of Materials Processing Technology*, vol. 91, no. 1, pp. 111-115, 1999. DOI:10.1016/S0924-0136(98)00398-7
- [13] Y. Tozawa, "Forming technology for raising the accuracy of sheet-formed products," *Journal of Materials Processing Technology*, vol. 22, no. 3, pp. 343-351, 1990. DOI:10.1016/0924-0136(90)90020-U
- [14] T. X. Yu, y L. C. Zhang. "Plastic bending: Theory and applications," vol. 2, 1996.
- [15] K. Roll, y K. Weigand, "Tendencies and new requirements in the simulation of sheet metal forming processes," *Computer Methods in Materials Science*, vol. 9, pp. 12-24. 2009.
- [16] I. Sarraf, y D. Green, "Prediction of DP600 and TRIP780 yield loci using Yoshida anisotropic yield function," *IOP Conference Series: Materials Science and Engineering*, 418, 012089. 2018. DOI:10.1088/1757-899X/418/1/012089
- [17] T. Uemori, S. Sumikawa, T. Naka, N. Ma, y F. Yoshida, "Influence of Bauschinger Effect and Anisotropy on Springback of Aluminum Alloy Sheets," *Materials Transactions*, vol. 58, no. 6, pp. 921-926. 2017. DOI:10.2320/matertrans.L-M2017812
- [18] R. Hill, "A theory of the yielding and plastic flow of anisotropic metals," *Proceedings of the Royal Society of London. Series A. Mathematical and Physical Sciences*, 193(1033), pp. 281-297. 1948. DOI:10.1098/rspa.1948.0045
- [19] W. F. Hosford, "A Generalized Isotropic Yield Criterion," *Journal of Applied Mechanics*, vol. 39, no. 2, pp. 607-609. 1972. DOI:10.1115/1.3422732
- [20] F. Ozturk, S. Toros, y S. Kilic, "Effects of Anisotropic Yield Functions on Prediction of Forming Limit Diagrams of DP600

- Advanced High Strength Steel.” *Procedia Engineering*, vol. 81, pp. 760-765. 2014. DOI:10.1016/j.proeng.2014.10.073
- [21] S. A., Haus, “Influência do efeito baushinger no retorno elástico em aços avançados de elevada resistência,” Ph.D. dissertation, Universidade federal do paraná. Brasil, 2011.
- [22] F. Barlat, y K. Lian, “Plastic behavior and stretchability of sheet metals. Part I: A yield function for orthotropic sheets under plane stress conditions,” *International Journal of Plasticity*, vol. 5, no. 5, pp. 51-66. 1989. DOI: 10.1016/0749-6419(89)90019-3
- [23] P. A. Eggertsen, y K. Mattiasson, “On constitutive modeling for springback analysis,” *International Journal of Mechanical Sciences*, vol. 52, no. 6, pp. 804-818. 2010. DOI:10.1016/j.ijmecs.2010.01.008
- [24] S. Konzack, R. Radonjic, M. Liewald, y T. Altan. “Prediction and reduction of springback in 3D hat shape forming of AHSS,” *Procedia Manufacturing*, vol. 15, pp. 660-667. 2018. DOI: 10.1016/j.promfg.2018.07.296
- [25] L. Jayaharia, J. Gangadhara, S. Kumar, y B. Balunaik. “Investigation of high temperature forming of ASS 304 using BARLAT 3-Parameter Model,” *Materials Today: Proceedings*, vol. 4, no. 2, pp. 799–804, 2017. DOI: 10.1016/j.matpr.2017.01.088
- [26] ASTM E8 / E8M-21, Standard Test Methods for Tension Testing of Metallic Materials, ASTM International, West Conshohocken, PA, 2021ASTM International, West Conshohocken, PA, 2016. DOI:10.1520/E0008_E0008M-21
- [27] ASTM E-517: Test Method for Plastic Strain Ratio r for Sheet Metal. ASTM International, West Conshohocken, PA, 2016. DOI:10.1520/E0517-19
- [28] ASTM E1245–03 Standard Practice for Determining the Inclusion or Second-Phase Constituent Content of Metals by Automatic Image Analysis. ASTM International, West Conshohocken, PA, 2016. <https://doi.org/10.1520/E1245-03R16>
- [29] Ansys licence academic (s. f.). 2020. Available: <https://www.ansys.com/academic>, Accessed on: Jul. 5, 2020.
- [30] R. A. Dos Santos, “Influência da força pós dobra e da geometria da ferramenta no retorno elástico em processos de dobramento de aços de alta resistência,” Ph.D. dissertation, Universidade federal do paraná. Brasil, 2013.



Rodolfo Rodríguez-Baracaldo, received the Bs. Eng in Mechanical Engineering (1997) from the Universidad Nacional de Colombia, the Ms degree in Mechanical Engineering (1999), and the PhD degree in Materials Engineering and Metallurgy (2008) from Polytechnic University of Catalonia. He worked for the Universidad Nacional de Colombia since 2000. Currently, he is a Full Professor in the Mechanical and Mechatronics Department, Faculty of Engineering. Head of “Innovation in manufacturing processes and materials engineering” research group. His research interests include Mechanical Metallurgy, Mechanical Properties of Advanced Materials, Metal Forming, and Computational Materials: Modeling and Simulation.
ORCID: <http://orcid.org/0000-0003-3097-9312>



Yeison Parra-Rodríguez, received the Bs. Eng in Mechanical Engineering (2011) from the Universidad Libre de Colombia, the Ms degree in Materials and Processes Engineering (2020) from Universidad Nacional de Colombia. He has worked in different manufacturing companies

in Colombia.

ORCID: <http://orcid.org/0000-0002-4264-5515>



José Manuel Arroyo-Osorio is Ph.D. in Mechanical Engineering (UNICAMP), M.Sc. in Problem-Based Learning for Sciences and Engineering (Aalborg University), M.Sc. in Systems Engineering (Universidad Nacional de Colombia), and B.Sc. in Mechanical Engineering (Universidad Nacional de Colombia). He currently works as Associate Professor at the Faculty of Engineering of the National University of Colombia in Bogotá. Its activities are concentrated in manufacturing processes, computer-aided manufacturing, and engineering education.

ORCID: <http://orcid.org/0000-0003-3636-8029>